

Numerical simulation of vortex-induced vibrations of a pair of cylinders

Luis Alberto Segovia González¹, Armando Miguel Awruch²

*Programa de Pós-Graduação em Engenharia Civil,
Universidade Federal do Rio Grande do Sul
Av. Osvaldo Aranha 99 - 3º Andar
Porto Alegre - RS - Brasil - 90035-190*

ABSTRACT

The 2-D numerical simulation of vortex-induced vibrations of two closely spaced parallel rigid circular cylinders, restrained by elastic springs and aligned in a normal direction with respect to the free stream flow, is presented in this work. Fluid-structure interaction is taken into account by a strong coupling based in equilibrium and compatibility conditions at the interfaces. A moving mesh, adjustable to the motion of the bodies, is included using an Arbitrary Lagrangean-Eulerian (ALE) description.

1. INTRODUCTION

A 2-D numerical simulation of vortex-induced vibration of a pair of cylinders arranged side by side in a normal direction to the free stream flow is presented in this work.

Practical applications of this simulation include wind-induced vibrations of groups of high rise buildings, free standing chimneys or cooling towers, bundles of electrical transmission lines, vibration of ducts in nuclear reactors, etc.

All the above mentioned cases are typical examples of structures surrounded by a fluid, where the deformations of the bodies are negligible in comparison with their deflections and, consequently, the structure may be idealized as a rigid body supported by elastic springs. This approach was first used by Kawahara et al. (1984) employing a two-step explicit scheme with selective lumping for the flow analysis.

The flow of a viscous incompressible fluid is analysed here with an explicit Taylor-Galerkin scheme using the Finite Element Method (FEM) for space discretization. Taylor-Galerkin schemes were used firstly by Donea (1984) and Donea et al. (1984) for advection-diffusion problems, by Laval & Quartapelle (1990) and Tabarrok & Su (1994) for unsteady incompressible flows and by Löhner et al. (1984), Morgan et al. (1991) and Peraire et al. (1988) in the context of high

¹ Professor Assistente

² Professor Titular

compressible flows and wave propagation problems. Later, this scheme was used by several others authors.

The dynamic equilibrium equations of the structure are solved using the standard Newmark's Method (Bathe (1996)).

Structure-fluid coupling is carried out considering displacement compatibility and equilibrium of forces at the interface, modifying structural mass and damping matrices and the load vector acting on the solid body.

Mesh movement is controlled by an Arbitrary Lagrangean-Eulerian (ALE) scheme, which is suitable for problems involving moving boundaries. A mixed Eulerian-Lagrangian description has been used by Hughes et al. (1981) for incompressible viscous flows and by Donea et al. (1982), Liu & Ma (1982) and Liu & Gvildys (1986) for fluid-structure interaction problems related to nuclear reactor power plants and sloshing problems. Löhner (1988) employed the ALE description for high compressible flows. This useful technique was later used by many authors in the field of Computational Fluid Dynamics as well as in Computational Structural Analysis.

Two examples show that the model is an efficient tool for the study of fluid-structure interaction problems such as vortex-induced vibrations.

2. GOVERNING EQUATIONS AND COMPUTATIONAL FORMULATION

The unsteady isothermal flow of a viscous and slightly compressible fluid is governed by the following system of differential equations (Kawahara et al. (1984))

$$\frac{\mathcal{I}}{\mathcal{I}t}(\mathbf{r}v_i) + \frac{\mathcal{I}}{\mathcal{I}x_j} \left[(\mathbf{r}v_i v_j) + p\mathbf{d}_{ij} - \mathbf{m} \left(\frac{\mathcal{I}v_i}{\mathcal{I}x_j} + \frac{\mathcal{I}v_j}{\mathcal{I}x_i} \right) \right] - \frac{\mathcal{I}}{\mathcal{I}x_i} \left(\mathbf{I} \frac{\mathcal{I}v_k}{\mathcal{I}x_k} \right) + \mathbf{r}f_i = 0 \quad (1)$$

(i, j, k = 1, 2) in Ω

$$\frac{\mathcal{I}p}{\mathcal{I}t} + c^2 \frac{\mathcal{I}}{\mathcal{I}x_j}(\mathbf{r}v_j) = 0 \quad (j = 1, 2) \quad \text{in } \Omega \quad (2)$$

with the corresponding boundary conditions

$$v_i = \bar{v}_i \quad (i = 1, 2) \quad \text{in } \Gamma_v \quad (3)$$

$$s_i = \left[-p\mathbf{d}_{ij} + \mathbf{m} \left(\frac{\mathcal{I}v_i}{\mathcal{I}x_j} + \frac{\mathcal{I}v_j}{\mathcal{I}x_i} \right) + \mathbf{I} \frac{\mathcal{I}v_k}{\mathcal{I}x_k} \right] n_j \quad (i, j, k = 1, 2) \quad \text{in } \Gamma_s \quad (4)$$

where v_i are the velocity components, p is the pressure, \mathbf{r} is the specific mass, f_i are the body force components, c is the velocity of propagation of sound, \mathbf{m} and \mathbf{I} are the molecular viscosity and bulk coefficient respectively, \bar{v}_i are prescribed values of the velocity components in \mathbf{G}_v , s_i are the components of the surface force in \mathbf{G}_s , n_i is the direction cosine of the outflow normal with respect to the axis x_i , \mathbf{d}_{ij} is the Kroenecker's delta and \mathbf{W} is the domain, with boundary $\mathbf{G} = \mathbf{G}_v \cup \mathbf{G}_s$.

The continuity equation (2) is obtained using the state equation

$$\frac{\mathcal{I}P}{\mathcal{I}\mathbf{r}} = c^2 \quad (5)$$

in the mass conservation equation given by

$$\frac{\mathcal{I}\mathbf{r}}{\mathcal{I}t} + \frac{\mathcal{I}(\mathbf{r}v_j)}{\mathcal{I}x_j} = 0 \quad (j=1,2) \quad (6)$$

Using the Taylor expansion of equations (1) and (2) up to the second order terms and applying the classical Buvnov-Galerkin scheme in the context of the FEM, the following expressions are obtained for the velocity components and pressure (Donea et al. (1982))

$$\left(\Delta V_{\sim i}\right)_{k+1}^{n+1} = \Delta t \left(M_{\sim L}^{-1}\right)^{n+1} \left\{ \left(L_{\sim ij} V_{\sim j} + G_{\sim i} P\right)^n + \frac{1}{2} \left[\left(L_{\sim ij} \Delta V_{\sim j}\right)_k + \frac{M_{\sim L} - M_{\sim L}}{\Delta t/2} \left(\Delta V_{\sim i}\right)_k + G_{\sim i} \left(\Delta P_{\sim k}\right) \right]^{n+1} + BT \right\} \quad (7)$$

(i, j = 1,2)

$$\left(\Delta P_{\sim k}\right)_{k+1}^{n+1} = \frac{\mathbf{r}c^2 \Delta t}{\Omega_e} \left[\left(G^T V_{\sim j}\right)^n + \frac{1}{2} \left(G^T \Delta V_{\sim j}\right)_k^{n+1} \right] \quad (j = 1,2) \quad (8)$$

where Δt is the time interval, Ω_e is the element domain, $M_{\sim L}$ is the lumped mass matrix, index n indicates the time step, while index k is the number of the iterations and BT denotes the boundary terms arising from the integration by parts of viscous and pressure terms.

Using four node isoparametric quadrilateral elements with bilinear interpolation functions for velocity components and with constant pressure over the element domain, matrices and vectors in expressions (7) and (8) are given by

$$M_{\sim L} = \int_{\Omega_e} \mathbf{r} \left(\Phi^T \Phi \right) d\Omega$$

$$G_{\sim i} = \int_{\Omega_e} \frac{\mathcal{I}\Phi^T}{\mathcal{I}x_i} d\Omega \quad (i = 1,2)$$

$$S_{\sim i} = \int_{\Omega_e} \Phi^T s_i d\Omega \quad (i = 1,2) \quad (9)$$

$$L_{\sim ii} = \int_{\Omega_e} \left[\mathbf{r} \left(\Phi^T V_{\sim m} \right) \left(\Phi^T \frac{\mathcal{I}\Phi}{\mathcal{I}x_m} \right) + (2\mathbf{m} + \mathbf{I}) \left(\frac{\mathcal{I}\Phi^T}{\mathcal{I}x_i} \frac{\mathcal{I}\Phi}{\mathcal{I}x_i} \right) + \mathbf{m} \left(\frac{\mathcal{I}\Phi^T}{\mathcal{I}x_j} \frac{\mathcal{I}\Phi}{\mathcal{I}x_j} \right) \right] d\Omega \quad (i, j, m = 1,2)$$

$$L_{\sim ij} = \int_{\Omega_e} \left[\mathbf{m} \left(\frac{\mathcal{I}\Phi^T}{\mathcal{I}x_i} \frac{\mathcal{I}\Phi}{\mathcal{I}x_j} \right) + \mathbf{I} \left(\frac{\mathcal{I}\Phi^T}{\mathcal{I}x_j} \frac{\mathcal{I}\Phi}{\mathcal{I}x_i} \right) \right] d\Omega \quad (i, j = 1,2)$$

where $\tilde{\Phi}$ is a vector containing the usual bilinear interpolation functions and index T indicates transposition. In the expressions for $L_{\tilde{ii}}$ and $L_{\tilde{ij}}$ we have $j = i + (-1)^{i+1}$.

With (7) and (8) the increments of velocity components at each node and pressure at element level are obtained. Nodal values of pressure may be calculated by a smoothing process employing local and global least-square techniques. As an explicit integration scheme is used, the local stability condition is given by (Kawahara et al. (1984))

$$\Delta t \leq \mathbf{a} \frac{\Delta x}{v + c} \quad (10)$$

where Δx is a characteristic element size, v is the velocity and \mathbf{a} is a safety factor.

Values of the velocity components in each node $V_{\tilde{i}}$ and values of pressure on each element $P_{\tilde{}}$ at time level $n+1$ are obtained with

$$V_{\tilde{i}}^{n+1} = V_{\tilde{i}}^n + \Delta V_{\tilde{i}}^{n+1} \quad (i=1,2) \quad (11)$$

$$P_{\tilde{}}^{n+1} = P_{\tilde{}}^n + \Delta P_{\tilde{}}^{n+1} \quad (12)$$

The equation of motion for the structure is given by

$$M_{\tilde{s}} \ddot{Y}_{\tilde{s}} + C_{\tilde{s}} \dot{Y}_{\tilde{s}} + K_{\tilde{s}} Y_{\tilde{s}} = Q_{\tilde{s}} \quad (13)$$

where $M_{\tilde{s}}$, $C_{\tilde{s}}$ and $K_{\tilde{s}}$ are the mass, damping and stiffness matrices respectively, $\ddot{Y}_{\tilde{s}}$, $\dot{Y}_{\tilde{s}}$ and $Y_{\tilde{s}}$ are the acceleration, velocity and displacement vectors respectively, and $Q_{\tilde{s}}$ is the load vector.

In this work each body has three degrees of freedom (displacements in the direction of each global axis and rotation around an axis normal to the domain Ω) and (13) is applied at the center of the body.

The momentum equation (1) may be written, in the context of the Galerkin scheme and the FEM, as a matrix equation given by

$$\begin{bmatrix} M_{\tilde{}} & 0 \\ 0 & M_{\tilde{}} \end{bmatrix} \begin{Bmatrix} \dot{V}_{\tilde{1}} \\ \dot{V}_{\tilde{2}} \end{Bmatrix} + \begin{bmatrix} L_{\tilde{11}} & L_{\tilde{12}} \\ L_{\tilde{21}} & L_{\tilde{22}} \end{bmatrix} \begin{Bmatrix} V_{\tilde{1}} \\ V_{\tilde{2}} \end{Bmatrix} = - \begin{Bmatrix} G_{\tilde{1}} P_{\tilde{}} \\ G_{\tilde{2}} P_{\tilde{}} \end{Bmatrix} + \begin{Bmatrix} S_{\tilde{1}} \\ S_{\tilde{2}} \end{Bmatrix} \quad (14)$$

or, in compact form

$$M_{\tilde{F}} \dot{V}_{\tilde{F}} + C_{\tilde{F}} V_{\tilde{F}} = -H_{\tilde{}} P_{\tilde{}} + S_{\tilde{}} \quad (15)$$

The compatibility condition at a node in the fluid-solid interface is

$$V_{\tilde{}} = T_{\tilde{}} \dot{Y}_{\tilde{}} \quad (16)$$

$$\underset{\sim}{T} = \begin{bmatrix} 1 & 0 & -t_2 \\ 0 & 1 & t_1 \end{bmatrix} \quad (17)$$

where t_1 and t_2 are the components of the distance from the node at the interface to the center of the body. Equation (16) indicates that the velocity at the center of the rigid body, transferred to the fluid-solid boundary, are equal to the fluid velocity at the same point.

The equilibrium condition at an element side in the fluid-solid interface is given by

$$\int_{\Gamma_e} \underset{\sim}{T}^T \underset{\sim}{S} d\Gamma = \underset{\sim}{Q} \quad (18)$$

where $\underset{\sim}{T}$ was defined in (16) and $\underset{\sim}{S}$ is a vector with their components defined in (4). Equation (18), together with (13), indicate that surface loads due to the fluid flow at the fluid-solid interface, transferred to the center of the rigid body, are in equilibrium with inertia, damping and elastic forces.

Considering expressions (13) to (18), the equation of motion of a body, taking into account the fluid-structure coupling, is given by

$$\left(\underset{\sim}{M}_S + \sum_m \underset{\sim}{R}^T \underset{\sim}{M}_F \underset{\sim}{R} \right) \ddot{\underset{\sim}{Y}} + \left(\underset{\sim}{C}_S + \sum_m \underset{\sim}{R}^T \underset{\sim}{C}_F \underset{\sim}{R} \right) \dot{\underset{\sim}{Y}} + \underset{\sim}{K}_S \underset{\sim}{Y} = - \sum_m \underset{\sim}{R}^T \left(- \underset{\sim}{M}_F \dot{\underset{\sim}{V}} - \underset{\sim}{C}_F \underset{\sim}{V} + \underset{\sim}{H} \underset{\sim}{P} \right) \quad (19)$$

where $\underset{\sim}{R}$ is obtained applying matrix $\underset{\sim}{T}$ for each node of the m finite elements having a common side with the fluid-solid interface.

As an example, assume that we are considering a quadrilateral element (e) with nodes **I**, **J**, **K**, **L**, with **I** and **J** lying at the fluid-solid interface and **K** and **L** have not any contact with the body boundary. In this case, matrix $\underset{\sim}{R}$ in (19) is given by

$$\underset{\sim}{R}^{(e)} = \begin{bmatrix} \underset{\sim}{T}^I \\ \underset{\sim}{T}^J \\ \underset{\sim}{T}^K \\ \underset{\sim}{T}^L \end{bmatrix} = \begin{bmatrix} 1 & 0 & -t_2^I \\ 0 & 1 & t_1^I \\ 1 & 0 & -t_2^J \\ 0 & 1 & t_1^J \\ 0 & 0 & 0 \\ 0 & 0 & 0 \\ 0 & 0 & 0 \\ 0 & 0 & 0 \end{bmatrix}$$

Solving (19) at the center of each body, the values of $\dot{\underset{\sim}{Y}}$ must be transferred to the fluid-solid interface in order to introduce boundary conditions for the fluid. The flow problem is analysed using expressions (7) to (12).

As the finite element mesh used for the flow simulation must follow the interface motion due to body oscillations, an Arbitrary Lagrangean-Eulerian (ALE) description is used. To introduce mesh movement it is necessary to modify advective terms in the momentum equation (1) taking

$\mathbf{r}v_i(v_j - w_j)$, where w_j are the components of the mesh velocity and consequently modifying matrix \tilde{L}_{ii} , given in (9).

The criterion used to compute the velocity components of each node I in the finite element mesh is (Donea et al. (1982)).

$$w_{i,I}^{n+1} = \frac{1}{N} \sum_{J=1}^N w_{i,J}^n + \frac{1}{10 \Delta t N^2} \sum_{J=1}^N d_{IJ}^n \sum_{J=1}^N \frac{\mathbf{d}_{i,J}^n - \mathbf{d}_{i,I}^n}{d_{IJ}^n} \quad (i = 1, 2) \quad (20)$$

where N indicates the number of nodes connected to node I through elements side or diagonals, d_{IJ}^n is the length of the segment IJ and $\mathbf{d}_{i,J}^n$ denote the displacement components of node J . In order to avoid undesirable mesh distortions, it is convenient to use together with (20) some restrictions such as (Giuliani (1982)).

$$w_{i,I} = -\mathbf{z} \left(\frac{\tilde{w}_{i,I}}{\tilde{w}_{i,I} - v_{i,I}} \right) v_{i,I} \quad \text{if} \quad \frac{\tilde{w}_{i,I}}{v_{i,I}} < 0 \quad (i=1,2)$$

$$w_{i,I} = \tilde{w}_{i,I} \quad \text{if} \quad 0 \leq \frac{\tilde{w}_{i,I}}{v_{i,I}} \leq 1 \quad (i=1,2) \quad (21)$$

$$w_{i,I} = \left[1 + \mathbf{z} \left(\frac{\tilde{w}_{i,I} - v_{i,I}}{\tilde{w}_{i,I}} \right) \right] v_{i,I} \quad \text{if} \quad \frac{\tilde{w}_{i,I}}{v_{i,I}} > 1 \quad (i=1,2)$$

where $\tilde{w}_{i,I}$ are obtained with expression (20), $v_{i,I}$ are the fluid velocity components and \mathbf{z} is a coefficient ($0 \leq \mathbf{z} \leq 1$).

3. EXAMPLES

3.1. Example 1

As a first example, in order to check the computational model, the open flow of a viscous fluid around an oscillating cylinder restrained by elastic springs with Reynolds number $Re = 1193$ is analysed. Geometrical characteristics and boundary conditions are shown in Figure 1. A finite element mesh with 2336 isoparametric quadrilateral elements and 2431 nodes, using bilinear shape functions for velocity components and constant pressure at element level, was employed.

The specific mass, shear viscosity, volumetric viscosity and sound speed for the fluid are, respectively

$$\begin{aligned} \mathbf{r} &= 1.32 \times 10^{-1} \text{ kg/m}^3 \\ \mathbf{m} &= 1.32 \times 10^{-2} \text{ kg/ms} \\ \mathbf{l} &= 0.00 \text{ kg/ms} \\ c &= 337.00 \text{ m/s} \end{aligned}$$

The undisturbed upstream velocity was assumed to be $\bar{v}_0 = 42.30 \text{ m/s}$

The solid body is characterized by the following geometrical and mechanical properties (mass, damping and stiffness, respectively) in x_2 direction

$$D = 2.82 \text{ m}$$

$$m_{22} = 84.43 \text{ kg}$$

$$c_{22} = 159.15 \text{ Ns/m}$$

$$k_{22} = 3.00 \times 10^4 \text{ N/m}$$

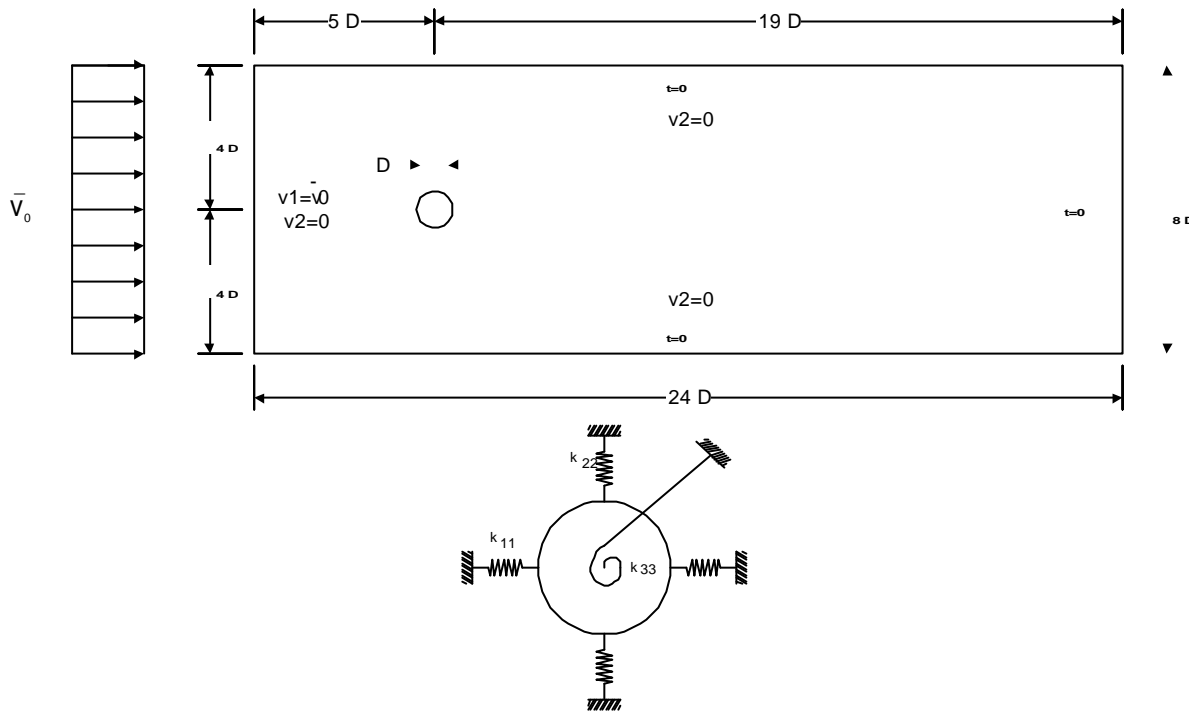


Figure 1: Geometrical characteristics and boundary conditions for the flow around an oscillating cylinder

Values of properties in x_1 direction are adopted such that oscillations in the longitudinal direction can be neglected.

The natural frequency, the dimensionless frequency and the damping coefficient in x_2 direction may be computed as follow

$$f_n = \frac{1}{2\pi} \sqrt{\frac{k_{22}}{m_{22}}} = 3.00 \text{ Hz} \quad \mathbf{w}_n = \frac{v_0}{f_n D} = 5.00 \quad \boldsymbol{\alpha} = \frac{c_{22}}{2\sqrt{m_{22}k_{22}}} = 0.05$$

The initial conditions consider the system at rest in $t = 0.00 \text{ s}$, and assume that suddenly the upstream velocity $\bar{v}_0 = 42.30 \text{ m/s}$ is applied.

The adopted time interval was $\Delta t = 1.00 \times 10^{-4} \text{ s}$

After 5.00 s the following mean values were found for the lift coefficient, pitching moment coefficient and drag coefficient respectively

$$C_L \approx 0.00$$

$$C_M \approx 0.00$$

$$C_D = 1.21$$

Mean values of the pressure coefficient and details of the stream lines are shown in Figure 2 and Figure 3, respectively.

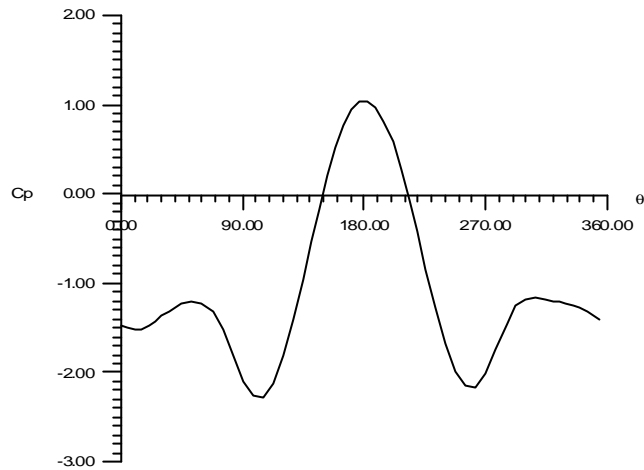


Figura 2: Mean values of the pressure coefficient

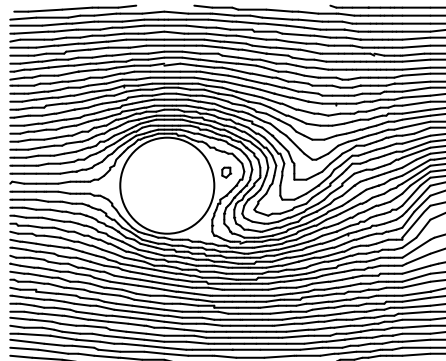


Figura 3: Details of the stream lines

Displacements of the center of the body, given in Figure 4, are similar to those obtained by Kawahara et al. (1984).

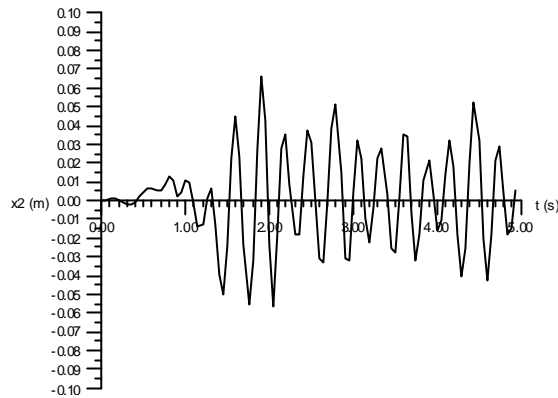


Figura 4: Displacements of the center of the cylinder

The Strouhal number $St = 0.22$ was calculated directly from the computed flow and is in good agreement with values reported by Kawahara et al. (1984), Schlichting (1979) and Zukauskas (1972).

3.2. Example 2

The mathematical model described in the previous section, was also applied to simulate vortex-induced vibrations for two closely spaced circular cylinders, arranged side by side perpendicular to the free stream flow direction, with Reynolds number of the flow $Re = 1193$. Geometrical characteristics and boundary conditions are shown in Figure 5.

The upstream velocity components were prescribed with the following values

$$\bar{v}_1 = 42.30 \text{ m/s}$$

$$\bar{v}_2 = 0.00 \text{ m/s}$$

and at the lateral boundaries the normal velocity component was prescribed with

$$\bar{v}_2 = 0.00 \text{ m/s}$$

The diameter and mechanical properties in x_2 direction (mass, damping and stiffness, respectively) of both cylinders were taken as

$$D = 2.82 \text{ m}$$

$$m_{22} = 84.43 \text{ kg}$$

$$c_{22} = 159.15 \text{ Ns/m}$$

$$k_{22} = 1.00 \times 10^4 \text{ N/m}$$

and values of properties in x_1 direction were adopted such that oscillations in the longitudinal direction can be neglected.

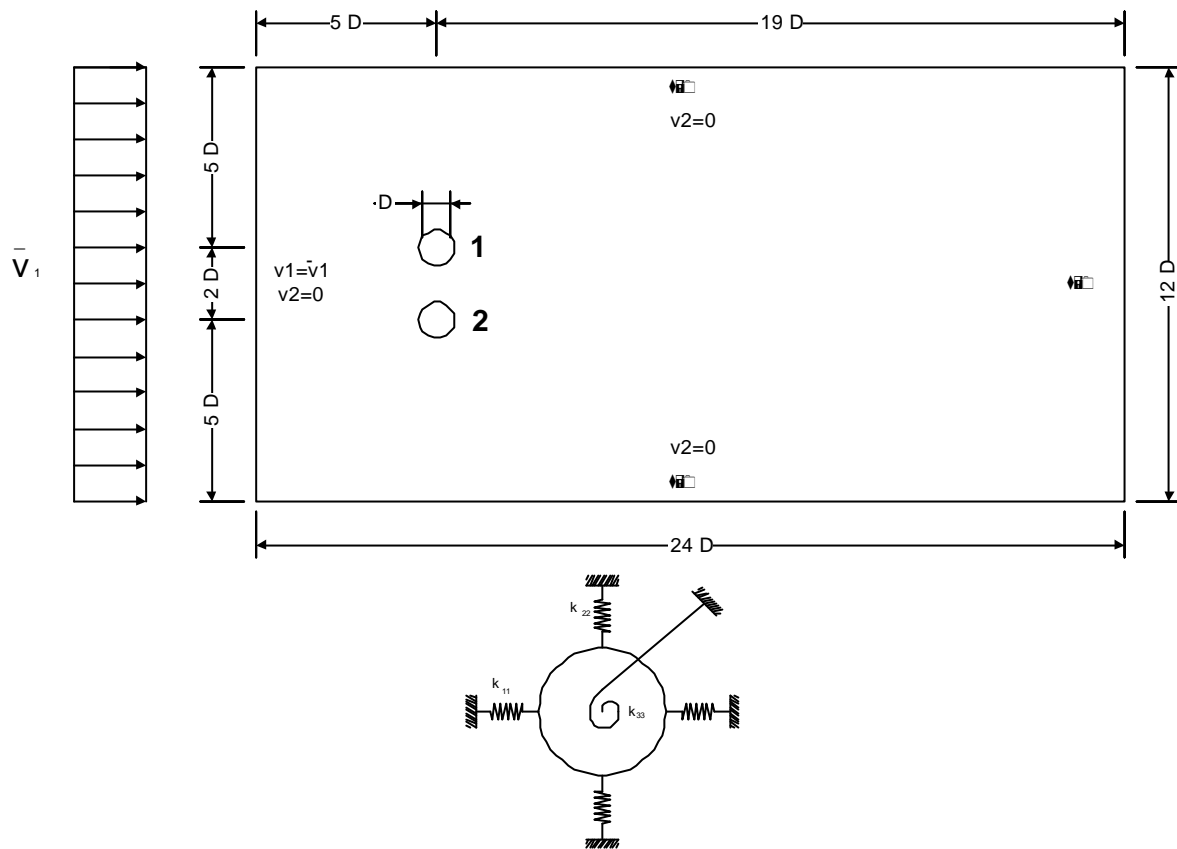


Figure 5: Geometrical characteristics and boundary conditions for the flow around a pair of oscillating cylinders

A mesh, depicted in Figure 6, with 5260 four node quadrilateral isoparametric elements and 5434 nodes was used to analyse this problem.

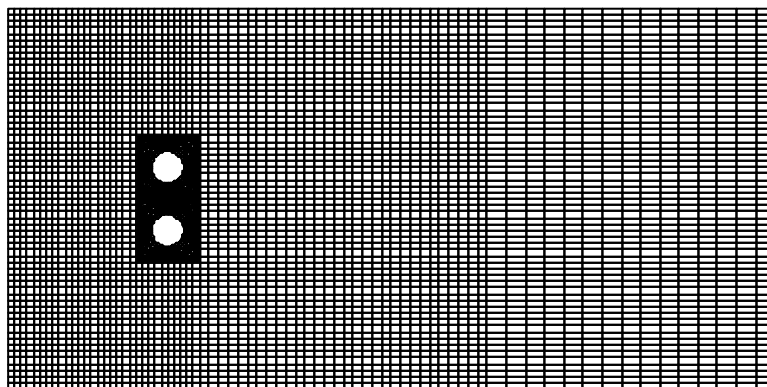


Figure 6: Finite element mesh

In Figure 7 details of the moving finite element mesh around cylinder 2 at $t = 3.90$ s. are shown, and in Figure 8 stream lines around both cylinders at $t = 3.00$ s

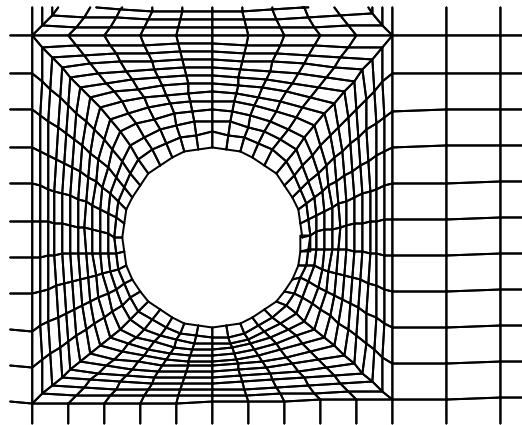


Figure 7: Moving finite element mesh around cylinder 2

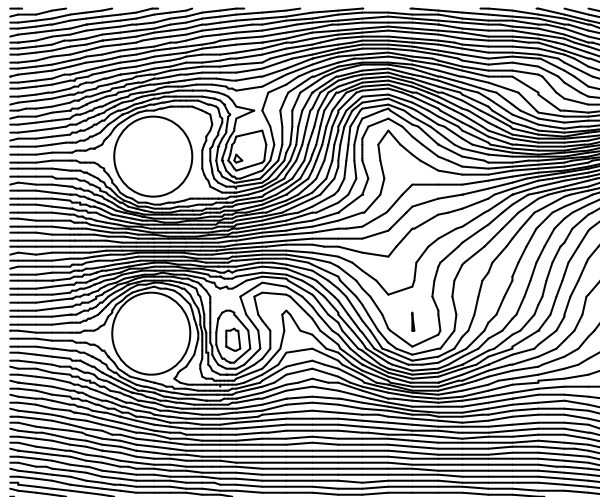


Figura 8: Detalhes of the stream lines

Transversal displacements of the center and mean values of the pressure coefficient for both cylinders can be observed in Figure 9 and 10 respectively.

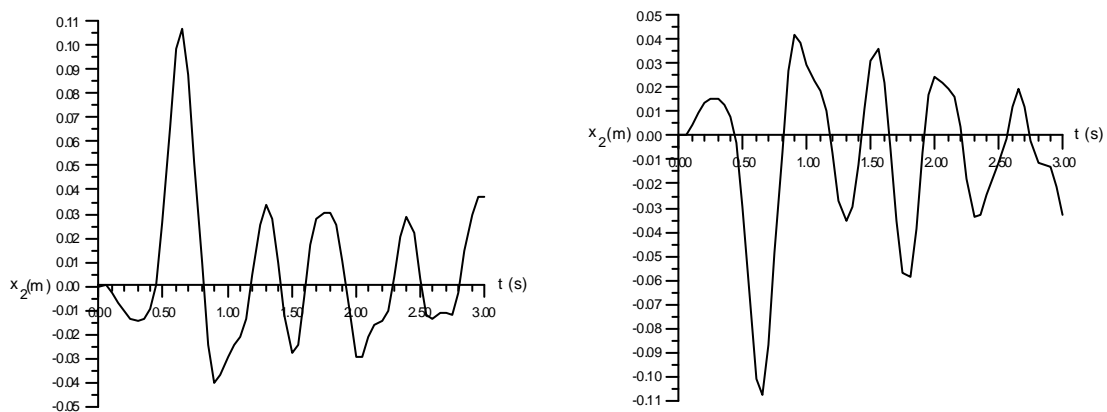


Figure 9: Perpendicular displacements of the center of cylinders 1 and 2

with respect to the free stream

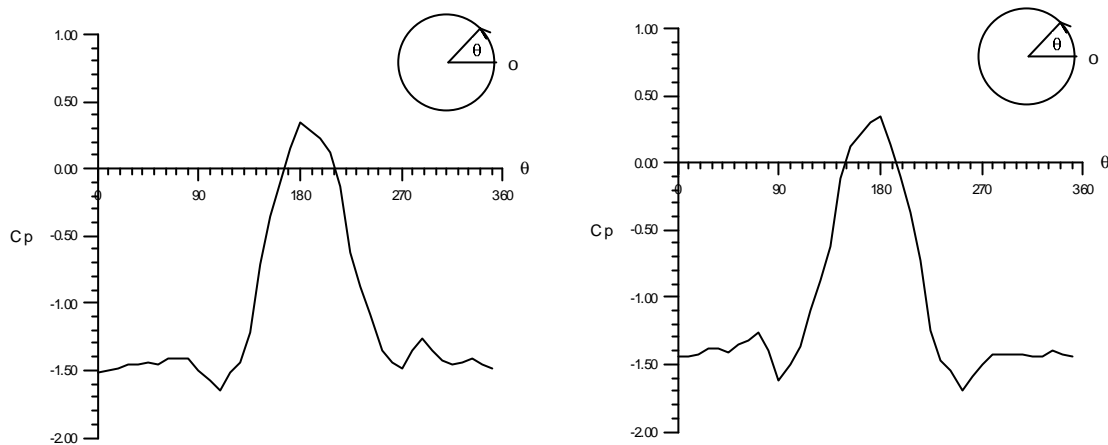


Figure 10: Mean values of the pressure coefficients for cylinders 1 and 2

Mean values of drag, lift and pitching moment coefficients were also obtained and are given by

$$\begin{array}{lll}
 C_{D_1} = 1.08 & C_{D_2} = 1.02 & C_{M_1} = -0.03 \\
 C_{L_1} = 0.22 & C_{L_2} = -0.24 & C_{M_2} = 0.03
 \end{array}$$

In all cases, mean values were calculated from time variation of instantaneous values. Results show good agreement with Zdravkovich (1977) and Price & Paidoussis (1984).

4. CONCLUSIONS

The encouraging results obtained in this work show the possibility to use the model described here as an efficient tool to study fluid-structure interactions problems, such as vortex-induced vibrations in an arbitrary arrangement of structures. Further developments to extend this computer code to 3-D, including a turbulence model as well, are being formulated and results will appear in future works.

5. REFERENCES

- Bathe, J. K. Finite Element Procedures. Prentice Hall, Henglewood Cliffs, N. J. (1996).
- Donea, J. A Taylor-Galerkin method for convective transport problems. *International Journal for Numerical Methods in Engineering*, **20**, 101-119 (1984).
- Donea, J.; Giuliani, S. & Halleux, J. P. An arbitrary lagrangean-eulerian finite element method for transient dynamic fluid-structure interactions. *Computer Methods in Applied Mechanics and Engineering*, **33**, 680-723 (1982).
- Donea, J.; Giuliani, S.; Laval, H. & Quartapelle, L. Time-accurate solution of advection-diffusion problems by finite elements. *Computer Methods in Applied Mechanics and Engineering*, **45**, 123-145 (1984).
- Giuliani, S. An algorithm for continuous rezoning of the hydrodynamic grid in arbitrary Lagrangian-Eulerian computer codes. *Nuclear Engineering Design*, **72**, 205-212 (1982).

Hughes, T. J. R.; Liu, W. K. & Zimmermann, T. K. Lagrangian-eulerian finite element formulation for incompressible fluid flows. *Computer Methods in Applied Mechanics and Engineering*. **29**, 329-349 (1981).

Kawahara, M.; Hirano, H. & Kodama, T. Two-step explicit finite element method for high Reynolds number flow passed through oscillating body. *Finite Elements in Fluids*. **5**, 227-262 (1984).

Laval, H. & Quartapelle, L. A fractional-step Taylor-Galerkin method for unsteady incompressible flows. *International Journal for Numerical Methods in Fluids*. **11**, 501-513 (1990).

Liu, W. K. & Gvildys, J. Fluid-structure interaction of tanks with eccentric core barrel. *Computer Methods in Applied Mechanics and Engineering*. **58**, 51-77 (1986).

Liu, W. K. & Ma, D. C. Computer implementation aspects for fluid-structure interaction problems. *Computer Methods in Applied Mechanics and Engineering*. **31**, 129-148 (1982).

Löhner, R. An adaptive finite element solver for transient problems with moving bodies. *Computers & Structures*. **10**, 303-317 (1988).

Löhner, R.; Morgan, K. & Zienkiewicz, O. C. The solution of non-linear hyperbolic equation systems by the finite element method. *International Journal for Numerical Methods in Fluids*. **4**, 1043-1063 (1984).

Morgan, K.; Peraire, J.; Peiro, J. & Hassan, O. The computation of three-dimensional flows using unstructured grids. *Computer Methods in Applied Mechanics and Engineering*. **87**, 335-352 (1991).

Peraire, J.; Peiro, J.; Formaggia, L.; Morgan, K. & Zienkiewicz, O. C. Finite element computations in three dimensions. *International Journal for Numerical Methods in Engineering*. **26**, 2135-2159 (1988).

Price, S. J. & Paidoussis, M. P. The aerodynamic forces acting on groups of two and three circular cylinders when subject to a cross-flow. *Journal of Wind Engineering and Industrial Aerodynamics*. **17** 329-347 (1984).

Schlichting, H. *Boundary Layer Theory*. 7^a Edn. Mc-Graw Hill, New York (1979).

Tabarrok, B. & Su, J. Semi-implicit Taylor-Galerkin element methods for incompressible viscous flows. *Computer Methods in Applied Mechanics and Engineering*. **117**, 391-410 (1994).

Zdravkovich, M. M. Review of flow interference between two circular cylinders in various arrangements. *Journal of Fluids Engineering*. **99**, 618-633 (1977).

Zukauskas, A. Heat transfer from tubes in cross flow. *Advanced in Heat Transfer*. **8**, 93-160 (1972).